RSC Advances

ROYAL SOCIETY OF CHEMISTRY

www.rsc.org/advances

Table of contents entry

Performance and potential problems of high power density zinc-nickel single flow batteries

Yuanhui Cheng[a,b], Xiaoli Xi[a,b], Dan Li[a], Xianfeng Li[a], Qinzhi Lai[a,*], Huamin Zhang[a,*]

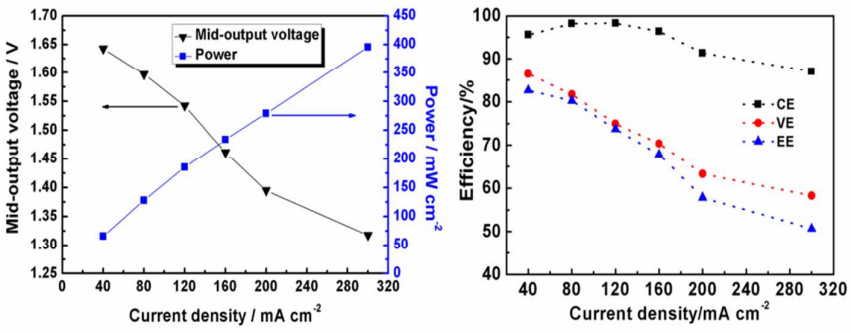

Though the investigation of battery performance and potential problems, we point out remaining issues and struggling directions of ZNBs.

Cite this: DOI: 10.1039/c0xx00000x

www.rsc.org/xxxxxx

Full paper

Performance and potential problems of high power density zinc-nickel single flow batteries

Yuanhui Cheng[a,b], Xiaoli Xi[a,b], Dan Li[a], Xianfeng Li[a], Qinzhi Lai[a,*], Huamin Zhang[a,*]

Received (in XXX, XXX) Xth XXXXXXXXX 20XX, Accepted Xth XXXXXXXXX 20XX

DOI: 10.1039/b000000x

High power density with high efficiency can realize rapid charge-discharge and reduce the cost of zinc-nickel single flow batteries, and is therefore of significant technological value. In this paper, the battery performance and potential problems have been investigated at high current density up to 300 mA cm^{-2}, which is the highest current density that has ever reached. The results show that coulombic efficiency firstly increases and then decreases with the current density increasing due to non-uniform distribution of electrode potential and side reactions. Positive electrode discharges deeply and zinc accumulates on the negative electrode at the end of the discharging process at high current density. The morphologies of deposited zinc vary from smooth, spongy to dendrite with the current density increasing. And the positive polarization is the critical obstacle to improve its performance at high current density. Based on these finding, we point out the remaining issues and struggling directions enabling high power density ZNBs without the substantial loss of cycle life.

1. Introduction

Zinc-nickel single flow battery (ZNB) is a promising energy storage device for improving the reliability and overall use of renewable energy due to its advantages of low cost, high efficient, long cycle life, high open circle potential (1.705 V) and high energy density [1-3]. The anode is zinc electrode with high electrode potential ($Zn(OH)_4^{2-} + 2e = Zn + 4OH^-$, -1.215 V vs. SHE, standard hydrogen electrode) and high specific capacity (820 mAh g^{-1}), which is widely used in zinc-based batteries[4, 5]. The cathode is a nickel hydroxide/nickel oxyhydroxide electrode ($Ni(OH)_2 - e + OH^- = NiOOH + H_2O$, 0.49V vs. SHE) that is diffusely employed in Ni-Cd and Ni-MH batteries[6-8]. And no membrane is needed between positive and negative electrodes, which simplifies the structure and reduces the cost compared to traditional two flowing electrolyte batteries. Different from traditional zinc-nickel batteries, the flowing electrolyte enhances proton transport at cathode and inhibits zinc dendrite at anode in ZNBs, which remarkably improves the energy efficiency and cycle life.

The energy may be generated or consumed in a short time, which requires the battery with high power density. In addition, the stack with high power density can reduce the cost of direct materials and thereby reduce the cost of flow batteries [9]. However, ZNB has suffered from large polarization resulted in low operating current density (below 20 mA cm^{-2}) and high cost for a long time [1, 10, 11]. Various efforts have been focused on improving its efficiency at high operating current density[3, 12-14]. With the development of cell structure, electrode material and structure, and electrolyte addictives, the polarization is dramatically reduced and the highest operating current density reaches 80 mA cm^{-2} with high energy efficiency (80%) [3, 14], but still cannot fulfill the requirement for rapid charge and discharge. The exchange current density for zinc deposition and dissolution is found to be as high as 370 mA cm^{-2} in alkaline solutions [15], which is much higher than the operating current density of ZNBs. Such, ZNB could be operated at several hundred milliampere per square centimeter theoretically. But so far, no study has been focused on the battery performance, potential problems and the critical obstacle for the improvement of battery performance at such high operating current density.

Here, the performance of ZNB at high current density (up to 300 mA cm^{-2}) has been investigated and the overpotentials of the positive and negative electrodes are quantitatively analyzed to search for the critical obstacle. The morphologies of deposited zinc and potential problems at high current densities have been analyzed. Based on these finding, we point out the remaining issues and struggling directions enabling high power density ZNBs.

2. Experimental section

2.1 Chemicals

Electrolyte was alkaline potassium zincate aqueous solution made of 0.4 mol dm^{-3} zinc oxide and 8 mol dm^{-3} potassium hydroxide. All chemicals were dissolved in deionized water without further treatment.

2.2 Electrochemical measurements

The schematic diagram of a single cell structure was shown in Fig. 1. The cell employed nickel hydroxide electrode (30 × 30 × 0.7 mm, Jiangsu Highstar Battery Manufacturing, China) with a capacity of 25 mAh cm^{-2} as positive electrode, nickel foam

[a]*Division of Energy Storage, Dalian National Laboratory for Clean Energy, Dalian Institute of Chemical Physics, Chinese Academy of Sciences, No.457 Zhongshan Road, Dalian 116023, (PR China). Fax: (+86) 0411-84665057; E-mail: zhanghm@dicp.ac.cn ; qinzhilai@dicp.ac.cn*

[b]*University of Chinese Academy of Sciences,Beijing 100039, (PR China).*

(30×30×2 mm, 420 g m^{-2}, 110 PPI, Changsha Lyrun Material Co., Ltd., China) as negative electrode and 8 mol dm^{-3} potassium hydroxide solution mixed with 0.4 mol dm^{-3} zinc oxide as electrolyte. The distance between positive electrode and negative electrode was 5 mm. The electrolyte was circulated through the cell by a pump with a rate of 19 cm s^{-1}. The cell was charged to 80% capacity based on the capacity of positive electrode and discharged to 0.8 V under the same constant current density from 40 mA cm^{-2} to 300 mA cm^{-2} demonstrated by Arbin BT-2000. The positive and negative potentials were measured with an Hg/HgO reference electrode (0.098 V vs. SHE) installed in the middle of the gap between two electrodes. All experiments are conducted at room temperature.

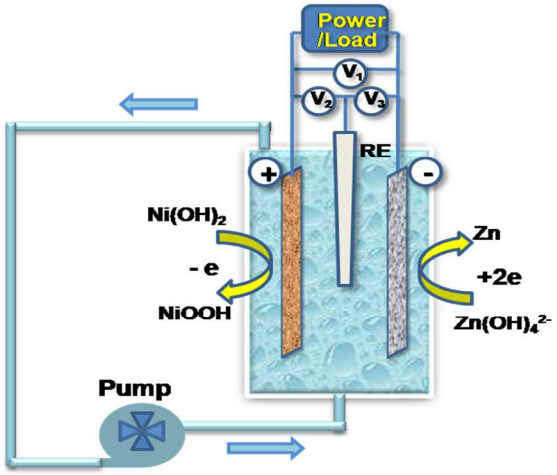

Fig. 1 The schematic diagram of a single cell structure.

2.3 SEM characterization

Negative electrodes were washed with deioned water and dried in a vacuum desiccator after charging to the capacity of 10 mAh cm^{-2} at various current densities (40 mA cm^{-2} to 300 mA cm^{-2}). The morphologies of deposited zinc were surveyed by scanning electron microscopy (SEM, JEOL JSM-6000, JEOL Ltd., Japan).

3. Results and discussion

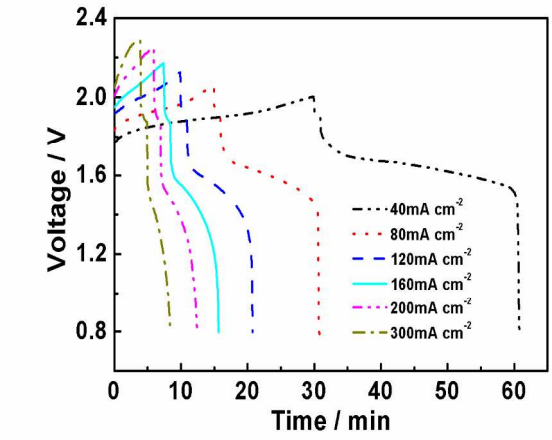

Fig. 2 Charge-discharge voltage curves at various current densities (40 mA cm^{-2} to 300 mA cm^{-2})

The charge-discharge voltage curve is an important parameter that can evaluate charge voltage and discharge voltage at high current density. The charge voltage increases and the discharge voltage declines with the current density increasing from 40 mA cm^{-2} to 300 mA cm^{-2} (Fig.2). Two critical indexes of battery application are the mid-output voltage (voltage value at the midpoint of the discharge period) and power density. The former decreases from 1.64 V to 1.32 V due to large polarization and the latter improves from 65.7 mW cm^{-2} to 395.3 mW cm^{-2} with a slope of 1.26 mW mA^{-1} from 40 mA cm^{-2} to 300 mA cm^{-2} (Fig.3). At 200 mA cm^{-2} for instance, the mid-output voltage (1.40 V) is higher than that of the mature vanadium-vanadium system (about 1.27 V) [16] and the recently proposed metal free quinine - bromine system (about 0.64 V) [17], the only two systems can operate at such high current density. As a result, the power density is the highest in flow battery families.

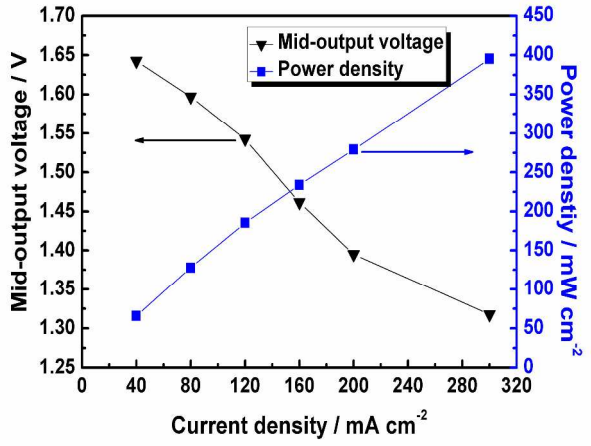

Fig. 3 Mid-output voltage and power density at various current densities (40 mA cm^{-2} to 300 mA cm^{-2}).

The coulombic efficiency (CE), voltage efficiency (VE) and energy efficiency (EE) are three important indexes of battery performance, which are defined by the ratios of discharge coulomb to charge coulomb, mean discharge voltage to mean charge voltage and discharge energy to charge energy respectively (Fig.4). There is a volcano type relation that CE is

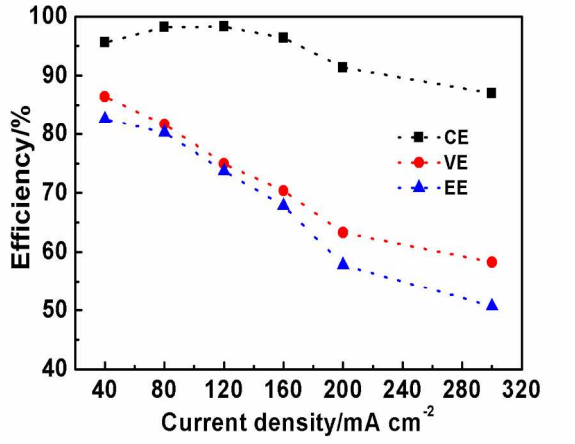

Fig. 4 Coulombic efficiency (CE), voltage efficiency (VE) and energy fficiency (EE) at various current densities (40 mA cm^{-2} to 300 mA cm^{-2}).

about 98.2% at 80 mA cm^{-2} and 120 mA cm^{-2}, and decreases with the current density decreasing to low current density or increasing to high current density. This is because that non-uniform distribution of potential on the negative electrode causes less utilized electrode surface for main reaction and more surface for hydrogen evolution at low current density. While at high current density, more oxygen produce on the positive electrode and hydrogen produce on the negative electrode, which both cause CE deteriorated. As a result, there is an optimum operating current density range to achieve high coulombic efficiency, which is between 80 mA cm^{-2} and 120 mA cm^{-2} at current operating conditions. While VE reduces from 86.4% to 58.3% with the current density increasing from 40 mA cm^{-2} to 300 mA cm^{-2} owning to its large polarization. As a result, EE decreases from 82.6% to 50.7%. This firstly reports the trends in efficiencies of ZNBs at ultrahigh current density up to 300 mA cm^{-2}.

The potentials of positive electrode and negative electrode are presented in Fig.5 and Fig.6. The potential of positive electrode increases upon charging and decreases upon discharging with the current density increasing. While the potential of negative electrode decreases upon charging and increases upon discharging due to large polarization (sluggish electrochemical reactions and large ohmic resistance). There is an interesting finding that negative electrode potential drops suddenly at the end of discharging process at low current density (40 mA cm^{-2} and 80 mA cm^{-2}), while that occurs on the positive electrode at high current density (120 mA cm^{-2} to 300 mA cm^{-2}). This indicates that negative electrode presents serious concentration polarization at the end of discharging process at low current density (40 mA cm^{-2} and 80 mA cm^{-2}), while that shifts to the positive electrode at high current density from 120 mA cm^{-2} to 300 mA cm^{-2}. Deposited zinc on the negative electrode dissolved completely at low current density (40 mA cm^{-2} and 80 mA cm^{-2}) and positive charged state NiOOH may not discharge completely. This was resulted from more electric charge consumed by side reaction (mainly hydrogen evolution) at negative side than that at positive side (mainly oxygen evolution). While at high current density (120 mA cm^{-2} to 300 mA cm^{-2}), zinc does not completely dissolve during discharging process and thereby accumulates on the negative electrode causing short circuit upon repeated charge-discharge cycles, and deep discharge occurs on the positive electrode which inevitably brings on deadly damnification on the cycle life of solid electrode. This stemmed from less electric charge consumed by side reaction at negative side (mainly hydrogen evolution) than that at positive side (mainly oxygen evolution) at high current density. As discussed above, the electric charge consumed by side reactions varies at both positive electrode and negative electrode at different operating current densities. And the asymmetry coulombic efficiencies of positive electrode and negative electrode will cause deterioration of battery stability and should be avoid as much as possible.

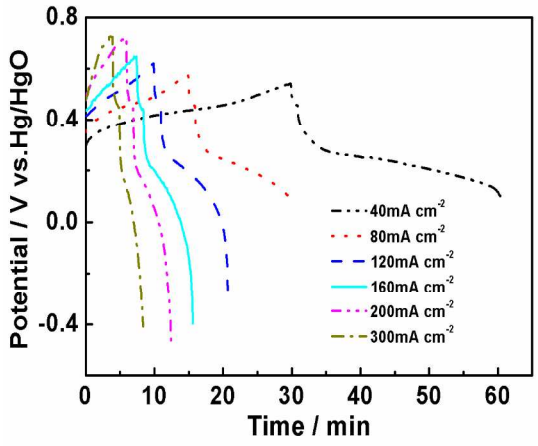

Fig. 5 Positive electrode potential at various current densities (40 mA cm^{-2} to 300 mA cm^{-2}).

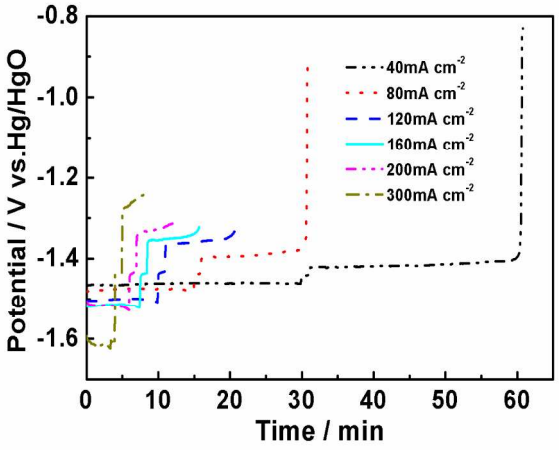

Fig. 6 Negative electrode potential at various current densities (40 mA cm^{-2} to 300 mA cm^{-2}).

Different operating current density will result in different morphologies of deposited zinc on the negative electrode as shown in Fig.7. With the current density increasing, the morphologies undergo smooth (Fig.7a), spongy (Fig.7b-e) and dendrite (Fig.7f) corresponding to current density of 40 mA cm^{-2}, 80 to 200 mA cm^{-2}, and 300 mA cm^{-2}. The smooth deposits are formed at low current density when the electrode reaction is controlled by electrochemical reactions. Dendritic deposits are formed when the rate of the electrode reaction is controlled by the mass transport of zincate species to the electrode surface. Similarly, the spongy deposits are formed at moderate reaction rate when the electrode reaction is controlled by the mix of mass transport of active species and electrochemical reactions. Such, the morphologies of deposited zinc, which transported from smooth, spongy to dendrite with the current density increasing, also have a strong relationship with the operating current density. At high current density, the mass transport of active species should be enhanced to depress dendritic deposition of zinc.

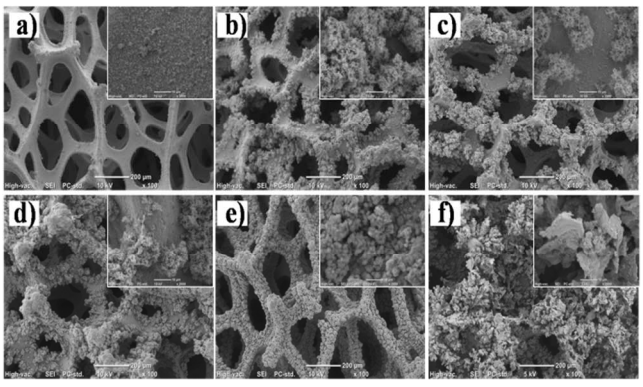

Fig. 7 Morphologies of deposited zinc on negative electrode at various current densities, a) 40 mA cm^{-2}, b) 80 mA cm^{-2}, c) 120 mA cm^{-2}, d) 160 mA cm^{-2}, e) 200 mA cm^{-2}, f) 300 mA cm^{-2}.

We calculated the overpotentials of positive electrode and negative electrode at various current densities (Fig.8, 40 mA cm^{-2} to 300 mA cm^{-2}) to find the critical obstacle for improving battery performance. The overpotential of positive electrode increases from 107.7 mV to 330.1 mV and that of negative electrode increases from 20.2 mV to 177.8 mV. The large overpotential of positive electrode is the prominent contributor that causes much side reactions, high charge voltage and low output voltage, and hinders the improvement of battery performance especially at high current density. Attempt should be tried to format high active positive electrode through the preparation of active materials and electrode structure to achieve high power density ZNBs.

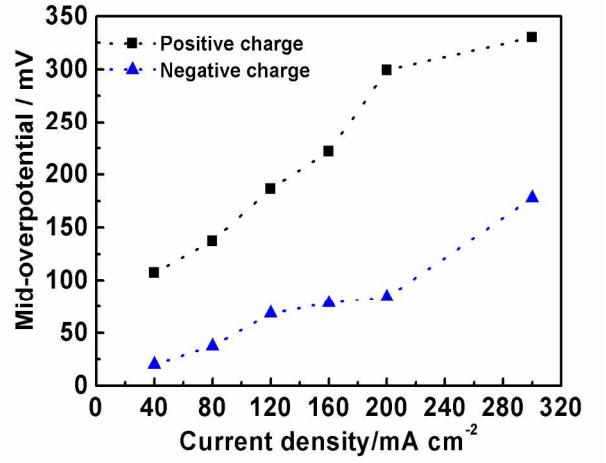

Fig. 8 Mid-overpotential of positive electrode and negative electrode at various current densities (40 mA cm^{-2} to 300 mA cm^{-2}).

Conclusions

During real charge-discharge cycling, there is an optimum operating current density range to achieve high coulombic efficiency at fixed conditions including cell structure, flow rate of electrolyte, concentration of electrolyte and so on. Similarly, the morphologies of deposited zinc, which transported from smooth, spongy to dendrite with the current density increasing, also have a strong relationship with the operating current density. At high current density, the mass transport of active species should be enhanced to depress dendritic deposition of zinc. Furthermore, the unmatched coulombic efficiencies of negative electrode and positive electrode may lead to the decrease in the cycle life of ZNBs, which has not roused enough attentions. And the large overpotential of the positive electrode is the critical obstacle to the improvement of battery performance at high operating current density. Elucidation of the performance and potential problems of ZNBs provides valuable information for its development and modification

Acknowledgement

This work is financial support by the National Basic Research Program of China (973 Program No. 2010CB227204).

References

1 J. Cheng, L. Zhang, Y. Yang, Y. Wen, G. Cao, X. Wang, Electrochem. Commun. 9 (2007) 2639-2642.
2 Y. Ito, M. Nyce, R. Plivelich, M. Klein, S. Banerjee, J. Power Sources, 196 (2011) 6583-6587.
3 Y. Cheng, H. Zhang, Q. Lai, X. Li, D. Shi, Electrochim. Acta, 105 (2013) 618-621.
4 F.R. McLarnon, E.J. Cairns, J. Electrochem. Soc.138 (1991) 645-664.
5 C. Xu, B. Li, H. Du, F. Kang, Angew. Chem. Int. Ed. 51 (2012) 933-935.
6 A.K. Shukla, S. Venugopalan, B. Hariprakash, J. Power Sources, 100 (2001) 125-148.
7 M. Oshitani, T. Takayama, K. Takashima, S. Tsuji, J. Appl. Electrochem. 16 (1986) 403-412.
8 Y. Wang, D. Cao, G. Wang, S. Wang, J. Wen, J. Yin, Electrochim. Acta, 56 (2011) 8285-8290.
9 V. Viswanathan, A. Crawford, D. Stephenson, S. Kim, W. Wang, B. Li, G. Coffey, E. Thomsen, G. Graff, P. Balducci, M. Kintner-Meyer, V. Sprenkle, J. Power Sources, 247 (2014) 1040-1051.
10 Y. Ito, M. Nyce, R. Plivelich, M. Klein, D. Steingart, S. Banerjee, J. Power Sources, 196 (2011) 2340-2345.
11 Y. Cheng, H. Zhang, Q. Lai, X. Li, Q. Zheng, X. Xi, C. Ding, J. Power Sources, 249 (2014) 435-439.
12 Y. Wen, T. Wang, J. Cheng, J. Pan, G. Cao, Y. Yang, Electrochim. Acta, 59 (2012) 64-68.
13 J. Cheng, Y. Wen, G. Cao, Y. Yang, J. Power Sources, 196 (2011) 1589-1592.
14 Y. Cheng, H. Zhang, Q. Lai, X. Li, D. Shi, L. Zhang, J. Power Sources, 241 (2013) 196-202.
15 J.O.M. Bockris, Z. Nagy, A. Damjanovic, J. Electrochem. Soc. 119 (1972) 285-295.
16 Q. Zheng, F. Xing, X. Li, T. Liu, Q. Lai, G. Ning, H. Zhang, J. Power Sources, doi: 10.1016/j.jpowsour.2014.04.148. (2014).
17 B. Huskinson, M.P. Marshak, C. Suh, S. Er, M.R. Gerhardt, C.J. Galvin, X. Chen, A. Aspuru-Guzik, R.G. Gordon, M.J. Aziz, Nature, 505 (2014) 195-198.